



# A new look at Apollo 17 LEAM data: Nighttime dust activity in 1976



Eberhard Grün <sup>a,b,\*</sup>, Mihály Horányi <sup>a</sup>

<sup>a</sup> Colorado Center for Lunar Dust and Atmospheric Studies, LASP, University of Colorado, Boulder, CO 80303, USA

<sup>b</sup> Max-Planck-Institute for Nuclear Physics, Heidelberg, Germany

## ARTICLE INFO

### Article history:

Received 3 November 2012

Received in revised form

8 October 2013

Accepted 14 October 2013

Available online 11 November 2013

### Keywords:

Lunar dust

LEAM

Apollo17 data analysis

## ABSTRACT

One of the unresolved enigmas from the Apollo era is the existence and characteristics of highly electrically charged dust floating above the lunar surface. Potential evidence for this hypothesized phenomenon came from the Lunar Ejecta and Meteorites (LEAM) experiment on Apollo 17. The LEAM instrument consisted of three sets of multi-coincidence dust sensors facing different directions. Recently, new arguments were raised (O'Brien, 2011) that the signals recorded by LEAM may be caused by interferences from heater current switching, which occurred most frequently near sunrise and sunset. In order to shed light on this controversy a new look into the LEAM data was initiated within the Colorado Center for Lunar and Dust and Atmospheric Studies (CCLDAS) team of NASA's Lunar Science Institute (NLSI). The purpose of this analysis is to verify the earlier analysis by Berg et al. (1975), and to find evidence for impacts of interplanetary meteoroids in the LEAM data available to us. A second goal is to find in the LEAM house keeping data evidence for excessive power switching and correlated signals in the LEAM science data. The original analysis by Berg et al. (1975) covered LEAM data during 22 lunations (~22 months) in 1973 and 1974. This data set is no longer available. For the present study, we had access to LEAM data for only about 5 lunations (140 days) in 1976. We analyzed the housekeeping data and observed excessive heating from about 24 h after sunrise until about 24 h before sunset. We defined sunrise and sunset when the LEAM temperature measurement reached  $-20^{\circ}\text{C}$  above which significant solar heating was apparent. For about 9 days around lunar noon the temperatures were so high that LEAM was switched off. During the times of excessive heating LEAM became very noisy. We limit our current analysis to about 24 h before sunset to about 24 h after sunrise when the LEAM temperatures were moderate  $<60^{\circ}\text{C}$ . This carefully analyzed data set of 74.6 days constitutes about 75% of the periods when LEAM was switched on in 1976. We did not find a systematic correlation between the infrequent heater switches and the occurrence of signals. During the lunar night the temperature was quite stable at approx.  $-25^{\circ}\text{C}$ . One TOF dust impact event and 19 potential dust events were recorded by all three sensors during the periods when the instrument was at moderate temperatures. This corresponds to an average event rate of 0.25/day. While nine events are compatible with a random occurrence the other 10 events occurred in three statistically significant bursts within about 1 h or less after another. Two bursts occurred within the middle of lunar night and one burst of three events was recorded by the West sensor just an hour before sunrise. The background rates are compatible with impact rates recorded by the dust instruments onboard the Pioneer 8 and 9 spacecraft in interplanetary space. Based on our definition of sunrise and sunset, the 1976 LEAM data do not indicate strongly enhanced dust activity at the terminator.

© 2013 Elsevier Ltd. All rights reserved.

## 1. Introduction

As part of the Apollo Lunar Surface Experiments Package (ALSEP) the Lunar Ejecta and Meteorites (LEAM) Experiment (Berg et al., 1973; Anon., 1975a, b, 1972) was deployed by the Apollo 17 astronauts on December 11, 1972 in the Taurus-Littrow area (Fig. 1) about 200 m west of the Landing Module (LM). Recently the Lunar Reconnaissance Orbiter (LRO) photographed the Apollo 17 landing site and the ALSEP station. In order to characterize the lunar dust

environment the LEAM experiment measured by three sensors the speed, radiant direction, momentum, and kinetic energy of incident particles. All three sensors were contained in a single box standing on 4 legs and were connected to the ALSEP central station by a cable. LEAM started measurements after the return of the landing module and continued to make observations for about 3.5 years.

## 2. The LEAM instrument

The goal of the LEAM experiment was to record micrometeoroids bombarding the lunar surface and to detect secondary

\* Corresponding author.

E-mail address: [eberhard.gruen@lasp.colorado.edu](mailto:eberhard.gruen@lasp.colorado.edu) (E. Grün).

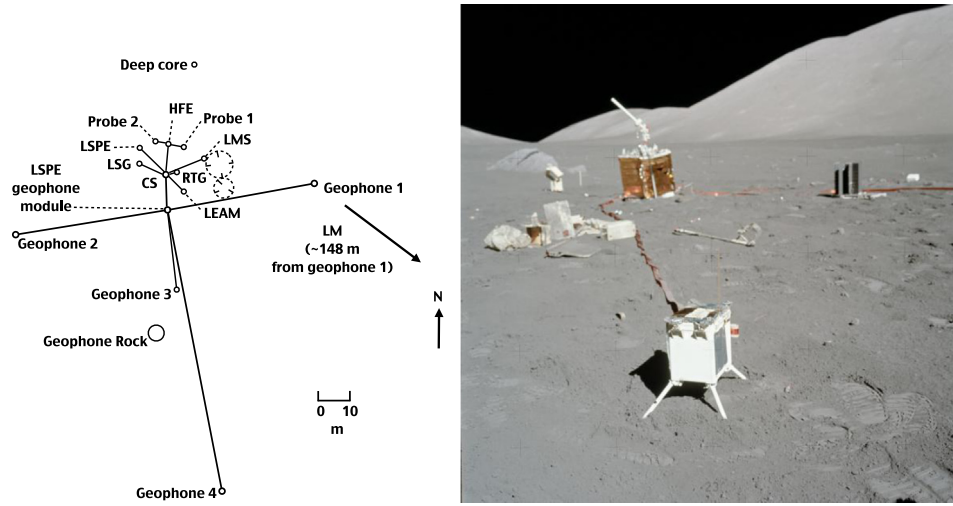


**Fig. 1.** Apollo 17 ALSEP station layout and photograph with the Lunar Ejecta and Meteorites (LEAM) Experiment in the foreground (NASA Apollo 17 photograph). Apollo 17 ALSEP comprised the Central Station (CS, upper central) with the antenna for communication with the Earth and connected by cables with the Radioisotope Thermoelectric Generator (RTG, upper right), and with the scientific instruments: Lunar Mass Spectrometer (LMS), Heat Flow Experiment (HFE), Lunar Surface Gravimeter (LSG), and Lunar Seismic Profiling Experiment (LSPE) with several Geophones.

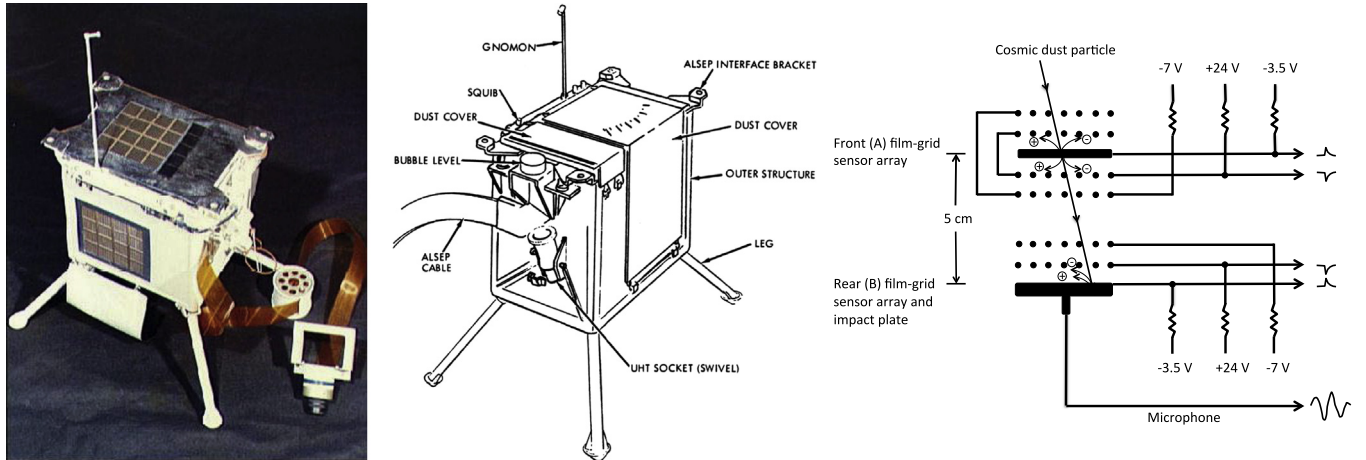


**Fig. 2.** Schematics of LEAM instrument (left), and one of its basic sensors elements (right) (from Berg et al., 1973). The front sensor consisted of  $0.3 \mu\text{m}$  thick aluminized polyethylene film and the rear sensor of a  $60 \mu\text{m}$  thick molybdenum sheet cemented to a quartz acoustical sensor plate (Berg and Richardson, 1969).

particles that had been ejected by bigger meteoroid impacts. Three classes of micron-sized cosmic dust particles were expected to be registered by LEAM: lunar ejecta, interplanetary dust from comets and asteroids, and interstellar grains.

The LEAM experiment is located at  $20.164^\circ\text{N}$  latitude and  $30.774^\circ\text{E}$  longitude on the moon (Berg et al., 1975). LEAM consisted of three sensor systems (Berg et al., 1973). The EAST sensor was pointed  $25^\circ$  North of East (Fig. 2) to include in its field-of-view the solar apex direction. The WEST sensor was pointing in the opposite direction as a control for the EAST sensor, while the UP sensor was parallel to the lunar surface and viewing particles coming from above. The field-of-view of each sensor is a square cone with a half-angle of approximately  $60^\circ$ . However, the mountainous terrain blocks about 60% of the field-of-view of both the EAST and WEST sensors.

The design and the expected performances of the LEAM experiment were similar to the dust sensors onboard the Pioneer 8 and 9 spacecraft (Berg and Richardson, 1969) that were launched into heliocentric orbits in 1967 and 1968, respectively (Berg and Grün, 1973). In a statistical analysis of the cosmic dust data from Pioneers 8 and 9 (Grün et al., 1973) demonstrated that the recorded events by these instruments constituted highly reliable measurements of dust in interplanetary space.

Each of the three sensor systems was comprised of two sets (front and a back) of  $4 \times 4$  basic sensor elements to determine the impacting particle's mass,  $m$ , and velocity vector,  $v$ . The sensors used a combination of thin plastic films and grids to measure the charge from the plasma cloud generated as the dust particles penetrated the film. The position of a penetration or an impact is determined by an array of four film and four perpendicular grid strips. This results in an array of 16 position elements. Two sets of sensors in a system were placed 5 cm apart, and a time-of-flight setup was used to determine the speed of an impacting dust particle. Each of the 16 front sensors were enabled to provide a start signal, and each of the 16 back sensors were designed to provide a stop signal for a total of 256 different combinations, enabling the determination of the velocity vector of the penetrating dust particles from the positions on the front and rear sensors and the elapsed time between start and stop signals. The only exception for this redundant arrangement was the WEST sensor 3, which lacked a front film-grid sensor. This sensor was designed to identify low-speed ejecta impacts that were expected not to penetrate the front film. Hence, the WEST sensor could not measure particle speed. Extensive laboratory calibrations were performed on these sensors using a 2 MeV electrostatic accelerator with particle masses in the range of  $10^{-13} < m < 10^{-9}$  g, and

**Table 1**

Mapping of Identifier Digital Number (DN) to the strips that recorded a signal.

Identifier DN	Strip 1	Strip 2	Strip 3	Strip 4
0	0	0	0	0
1	1	0	0	0
2	0	1	0	0
3	1	1	0	0
4	0	0	1	0
5	1	0	1	0
6	0	1	1	0
7	1	1	1	0
8	0	0	0	1
9	1	0	0	1
10	0	1	0	1
11	1	1	0	1
12	0	0	1	1
13	1	0	1	1
14	0	1	1	1
15	1	1	1	1

velocities up to 25 km/s. From these calibration tests it was determined that the signal amplitude is proportional to  $mv^{2.6}$ . The pulse height amplitudes (PHA) from the film-grid sensors were sorted in the (logarithmic) range from 0 to 7. In addition, the back impact plate was attached to a microphone with an acoustic signal proportional to the momentum of the grain.

Data readout is initiated by an impact event involving the "A" (front) film and/or the "B" (rear) film and/or the microphone. An impact signal received by the one or more of the front film strips is amplified and pulse-height analyzed. This signal is also used to identify the strip that recorded the signal (Table 1) and to increment the front film accumulator. In case a signal is recorded in coincidence by one or more front collector grid strips this front collector is identified and the information is added to the data.

The LEAM dust instrument implements controls to identify noise from dust impacts (Berg et al., 1973). These controls constituting one quarter (Lynn Lewis, private communication) of the total sensor area were exposed to the same "environment" as the active or main sensors. The control film and grid are "potted" in an epoxy resin, isolating them from the products of ionization caused by impacts upon their area (i.e., electrons and ions generated by hypervelocity impacts upon the epoxy cannot be collected upon the grids or films). The resin coat does not, however, constitute a shield from electromagnetic radiation. A microphone control is attached in the lower right corner of the rear plate having one fifteenth the effective area of the main microphone plate. More details and a block diagram of the electronics are given in Berg et al. (1973) and Anon. (1975a,b, 1972).

Test pulses are initiated either automatically or by command. High and low amplitudes pulses are alternately fed to the input of all amplifiers in order to check their condition. Front film sensor pulses and rear film sensor pulses are appropriately spaced to enable the monitoring of the time-of-flight electronics.

### 3. Previous data analysis

Once LEAM started to operate it became clear that its observations contradicted expectations. Based on previous measurements in interplanetary space by Pioneer 8 and 9, for example, the expected rate of interplanetary dust particles was a few impacts per day. Instead, LEAM registered up to hundreds of impacts per day, which swamped any signature of the expected primary impactors of either interplanetary or interstellar origin. Most puzzling was the fact that these events registered in the front film only, but frequently with the maximum possible pulse-height

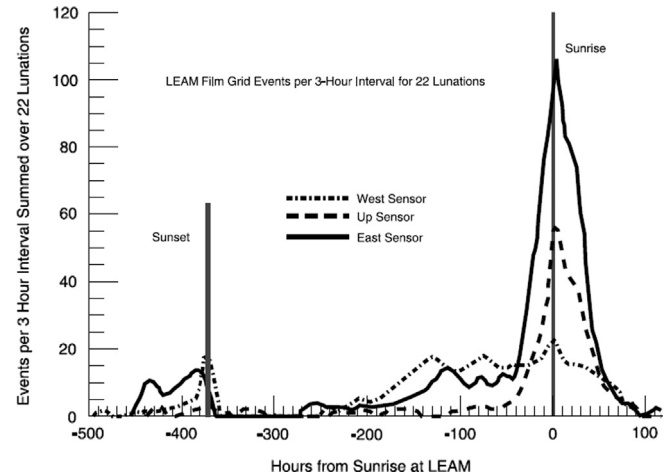


**Fig. 3.** Number of events recorded by the three LEAM sensors per 3-h intervals averaged over 22 lunations (Berg et al., 1975). The EAST and WEST sensors measured an approximately constant rate with constant PHA, while the UP sensor registered a declining rate after about 20 months on the lunar surface. From about 100 h after sunrise to about 100 h before sunset the instrument was switched off due to excessive solar heating.

amplitude (PHA) number of 7. Additionally, the LEAM operating temperature exceeded its predicted maximum value of  $\sim 60^{\circ}\text{C}$  at lunar noon, indicating possible thermal problems that were initially believed to be responsible for generating noise in the electronics, and possibly responsible for the elevated impact rates. This was supported by the correlation of the elevated impact rates with the passage of the terminator, both at sunrise and at sunset. As data accumulated, a systematic behavior was recognized. The sunrise terminator event rate started to increase shortly after local midnight at the site, and persisted for a period of approximately 60 h after sunrise – after this time the instrument was switched-off due to excessive solar heating. In this period the rates were up to 100 times higher than the normal background rates (Berg et al., 1975). Fig. 3 shows the number of dust impacts onto LEAM per 3-h period, integrated over 22 lunar days.

A new picture emerged to replace the high temperature electronics explanation: LEAM was registering slow moving, highly charged lunar dust particles. There were two subsequent studies done to verify this point: a theoretical work to model the response of the electronics (Perkins, 1976), and an experimental study of the LEAM flight spare (Bailey and Frantsvog, 1976). The results of the sensor modeling and circuit analysis showed that charged particles moving at velocities  $< 1 \text{ km/s}$  do produce large PHA responses via induced voltages on the entry grids, as opposed to signals from impact generated plasmas. This explains why the rear films remained silent even though the front sensor seemed to be hit by an energetic dust grain. The experimental study had a similar conclusion: extremely slow moving particles ( $v < 100 \text{ m/s}$ ) generate a LEAM response up to and including the maximum PHA of 7 if the particles carry a positive charge  $Q > 10^{-12} \text{ C}$ . Both of these studies suggest that the LEAM events are consistent with the sunrise/sunset-triggered levitation and transport of slow moving, highly charged lunar dust particles. Assuming a daytime surface potential of  $+5 \text{ V}$ , the LEAM measurements indicate grain sizes on the order of a millimeter in radius!

### 4. Purpose of the renewed LEAM data analysis

The purpose of this analysis is to repeat the analysis of early LEAM data from 1973 and 1974 by Berg et al. (1975) with data from 1976 and to find evidence for impacts of interplanetary meteoroids

in the LEAM data available to us. A second goal is to find in the ALSEP and LEAM housekeeping data evidence for the claim by O'Brien (2011) that the LEAM results published previously were false and could be explained by excessive power switching and correlated signals in the LEAM science data. O'Brien (2011) suggests that

- No impacts of interplanetary meteoroids have been detected.
- The majority of observed signals occurred in statistically highly improbable bursts of 2, 3, or 4 events within 3 h.
- The recorded signals were caused by interferences from heater current switching which occurred most frequently near sunrise and sunset.

The LEAM principal investigator Otto Berg and ALSEP engineers strongly opposed this view. In order to shed light on this controversy a new look into LEAM data was initiated within the NLSI/CCLDAS project.

## 5. The 1976 LEAM data set

As part of NASA's lunar data recovery project the Missing ALSEP Data Focus Group provided us with 140 days of LEAM data from 1976 (day 61–200, i.e. March–September) corresponding to about 5 lunations in 287 files. Each file contains a list of lines of 41 words each (totaling ~4 Million lines): 4 words Date/Time information, 1 word Main Frame counter, 31 words LEAM Science Data, and 5 words LEAM HK values. In a first step we identified gaps (totaling about 7 days) and removed overlaps in the data.

Based on Anon. (1975b, 1972) we extracted the relevant LEAM housekeeping and science data. The ALSEP data were transmitted at the normal data rate of 1060 bps. Each ALSEP Main Frame (MF) consists of 64 10-bit words. Word 31 and Word 39 is the LEAM science data and Word 33 is the LEAM House Keeping (HK) data.

A complete LEAM Science Data Set (Table 2) comprises 100 bits (10 ALSEP words). They are contained in 5 consecutive MFs; i.e. every 3 s a LEAM Science Data Set is transmitted. The LEAM Science Data Set contains identifiers (ID), pulse-height amplitudes (PHA), counter (Accumulator) and elapsed time data for the various sensors; it follows the scheme described by Berg and Richardson (1969) of the Pioneer 8/9 instruments. Sensor 1 (UP sensor) contains a front film sensor and a rear collector to which a microphone is attached. Sensor 2 (EAST sensor) has the same data structure. The WEST Sensor 3 contains only a rear collector section and, therefore, has no elapsed time measurement. The WEST Sensor implements two microphones: the main and a secondary microphone connected only to 1/15th of the impact target area. There is additional status information in the LEAM science data set (Table 2).

The Digital Number (DN) of the strip identifier ID represents the four sensor strips are listed in Table 1.

Ninety MFs cover all 90 different ALSEP HK words. Of specific interest for LEAM are the ALSEP HK words 83, 84, 85; they contain 5 LEAM HK channels each sub-commutated in word 83 and 84, and the ALSEP powered "LEAM Electric Survival temperature" contained in word 85.

LEAM HK Data Set (Table 3) comprises the 10 LEAM HK measurement channels. Each LEAM HK channel is digitized with 8 bits (DN: 0–255). The data rates for LEAM science and HK data are summarized in Table 4.

## 6. Housekeeping data analysis

Several ALSEP HK measurements monitor the thermal environment. Sunrise, sunset, and periods of solar illumination are clearly

**Table 2**  
LEAM science data set.

Meas. no.	Measurement name	ALSEP word	MF	Bits	LEAM word
<b>Sensor 1 (UP sensor)</b>					
DJ-1	Front film ID	31	1	1–4	1
DJ-2	Front film PHA	31	1	5–7	1
DJ-3	Front film accumulator	31	1	8–10	1
DJ-4	Rear film ID	39	1	1–4	2
DJ-5	Rear film PHA	39	1	5–7	2
DJ-6	Rear film accumulator	39	1	8–10	2
DJ-7	Front collector ID	31	2	1–4	3
DJ-8	Microphone PHA	31	2	5–7	3
DJ-9	Microphone accumulator	31	2	8–10	3
DJ-10	Rear collector ID	39	2	1–4	4
DJ-11	Elapsed time	39	2	5–10	4
<b>Sensor 2 (EAST sensor)</b>					
DJ-12	Front film ID	31	3	1–4	5
DJ-13	Front film PHA	31	3	5–7	5
DJ-14	Front film accumulator	31	3	8–10	5
DJ-15	Rear film ID	39	3	1–4	6
DJ-16	Rear film PIIA	39	3	5–7	6
DJ-17	Rear film accumulator	39	3	8–10	6
DJ-18	Front collector ID	31	4	1–4	7
DJ-19	Microphone PHA	31	4	5–7	7
DJ-20	Microphone accumulator	31	4	8–10	7
DJ-21	Rear collector ID	39	4	1–4	8
DJ-22	Elapsed time	39	4	5–10	8
<b>Sensor 3 (WEST sensor)</b>					
DJ-23	Film ID	31	5	1–2	9
DJ-24	Collector ID	31	5	3–4	9
DJ-25	Film PHA	31	5	5–7	9
DJ-26	Film accumulator	31	5	8–10	9
DJ-27	Secondary microphone accum.	39	5	1–2	10
DJ-30	Main microphone PHA	39	5	5–7	10
DJ-31	Main microphone accumulator	39	5	8–10	10
<b>General LEAM channels</b>					
DJ-28	Analog data sync ID BIT	39	5	3	10
DJ-29	Heater status	39	5	4	10

**Table 3**  
LEAM HK data set.

Meas. no	ALSEP word	SUBCOM seq.	Measurement name
AJ-1	83	1	+5 V Supply
AJ-2	83	2	Sensor dust covers status
AJ-3	83	3	Mirror dust cover status
AJ-4	83	4	Power supply monitor
AJ-5	83	5	Bias voltages monitor
AJ-6	84	1	Up microphone temp
AJ-7	84	2	East microphone temp
AJ-8	84	3	West microphone temp
AJ-9	84	4	Central electronic temp
AJ-10	84	5	–5 V Supply
	85	n/a	LEAM elec. survival temp

visible during the five lunations (lunar days) in 1976. The curves of some temperature measurements (e.g. ALSEP HK word 28 AT-4 Thermal Plate-2 Temp) indicate close control within a narrow temperature range by heaters and/or active radiators while others (e.g. ALSEP HK word 27 AT-1 Sunshield-L Temp) display wide temperature range with obviously little or no control. Similarly, the ALSEP powered temperature sensor "LEAM Elec. Survival Temp." (Fig. 4, ALSEP HK word 85) displays a wide range of temperatures measured within the instrument electronics. Since no calibration of the HK channels was available to us we generally display digital number (DN) values. By comparison with LEAM

temperatures reported by Berg et al. (1973) during the initial 3 lunations an approximate temperature scale can be established. Transmission gaps and transmission errors cause some gaps and outliers in the otherwise smooth temperature history. The LEAM temperature reached values beyond +60 °C during lunar day while it fell down to approx. -25 °C during lunar night (Table 5). We limit our initial analysis to periods when the LEAM temperatures were moderate (Fig. 4).

Ephemeris data like sunrise and sunset times were calculated in Earth date and GMT for each ALSEP station by the ALSEP Experiments Operation Room at JSC Mission Control (Lynn Lewis, personal communication, 2011). These times are similar to the times when the LEAM Electronics Survival Temperature reached the value of 20 DN ( $\sim -20$  °C) when significant heating by solar illumination started or declined, respectively (Table 5). Our analysis of LEAM data was restricted to lunar night from approximately 17 h before sunset to approximately 30 h after sunrise when LEAM Electronic Survival Temperature was below +60 °C.

The instrument powered HK measurements (Fig. 5) display a breakdown of the measurements for about 9 days around lunar

noon indicating an automatic switch-off of the instrument due to excessive heating. This behavior was already reported by Berg et al. (1973). Already before and after LEAM switched off (at the time when the Electronic Survival Temperature exceeded 187 DN) the +5 and -5 V Supply and other status measurements displayed deviation from their static values, indicating that the instrument left its nominal state. On request from the LEAM investigator during the fifth lunation in 1976 the instrument was not switched-off during the lunar day (Lynn Lewis, personal communication, 2011).

The LEAM powered Central Electronic Temperature shows generally larger DN values as the ALSEP powered LEAM Electronics Survival Temperature (Fig. 5 right) especially during the morning temperature rise. This effect may be due to temperature instability of the LEAM HK electronics.

**Table 5**

Times of sunrise and sunset in decimal days of 1976 (from Apollo 17 1976 Ephemeris Data, Lynn Lewis, personal communication). Additionally, we give the times when the measurements of the Electronic Survival Temperature indicated -20 °C (20 DN, Fig. 4) and +60 °C (187 DN). Lunation number count from start of mission in 1972.

Lunation number	Sunrise	Sunset	$T = -20$ °C	$T = +60$ °C	Excess temp. start in morning	Excess temp. stop in evening
41	66.042	80.834	66.486	81.101	67.451	80.159
42	95.584	110.375	96.043	110.620	97.009	109.615
43	125.084	139.875	125.554	140.097	126.637	139.048
44	154.584	169.334	154.714	169.550	156.175	168.468
45	184.042	198.792	184.516	198.970	185.670	198.000

**Table 4**  
ALSEP and LEAM data rates.

Data set	Data structure	Time (s)	Frequency ( $d^{-1}$ )
ALSEP main frame (MF)	64 10-bit words	0.603774	143,100
LEAM science data set (SDS)	31 1 to 6-bit words in 5 MFs	3.01887	28,620
LEAM HK data set	Ten 8-bit words in 450 MFs	271.698	318

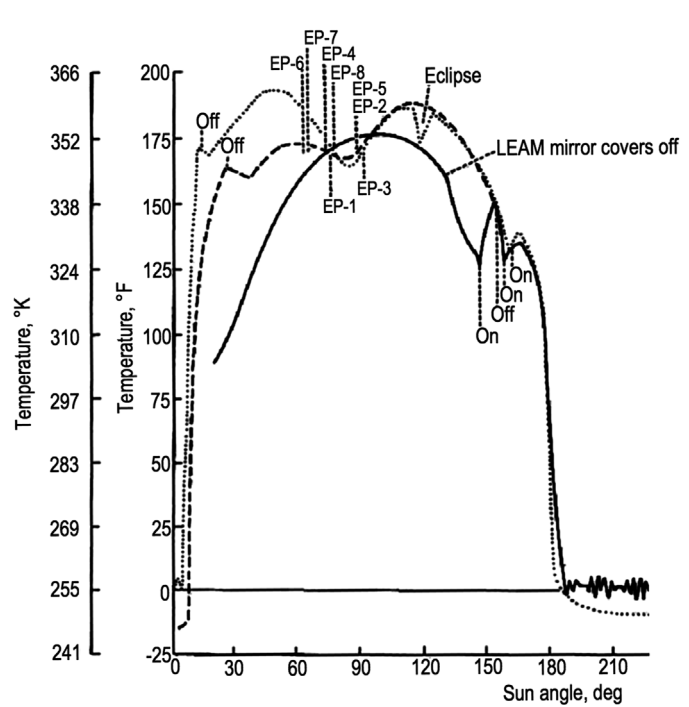
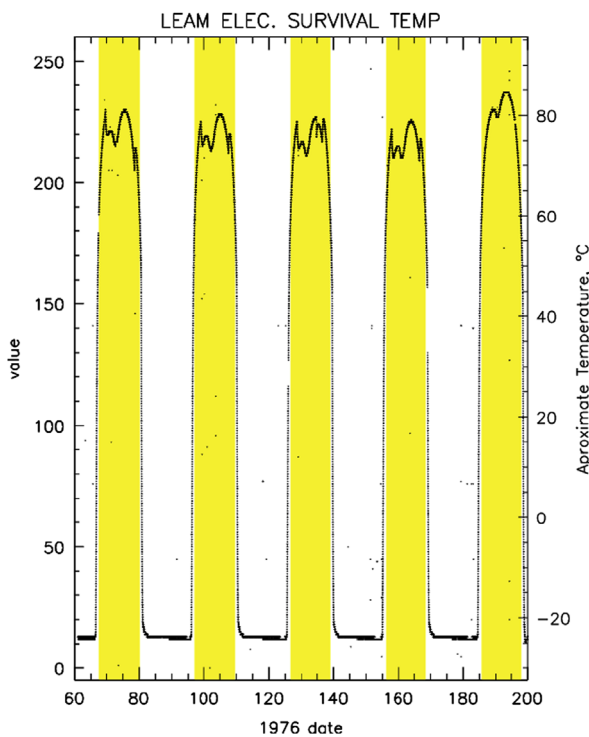


**Fig. 4.** ALSEP HK word 85: LEAM Electronics Survival Temperature in 1976 (left) and in 1973 at the beginning of LEAM operation (Berg et al., 1973, right). This temperature sensor is powered by ALSEP. The yellow bars indicate periods when LEAM temperatures exceeded 60 °C (187 DN) during lunar noon. These periods were excluded in our analysis. The right figure shows the temperature history during the first 3 lunations as function of sun angle (90° is lunar noon, from Berg et al., 1973); solid line: first lunation, dotted: lunation two, and dashed: lunation three. Various ALSEP and LEAM commanded events are indicated. (For interpretation of references to color in this figure legend, the reader is referred to the web version of this article.)

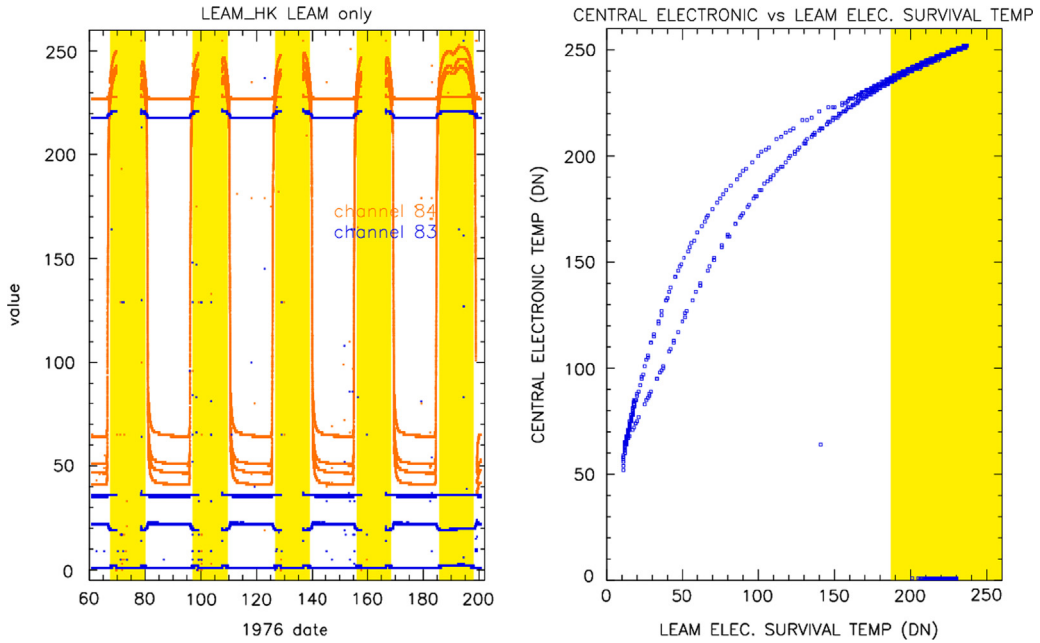


**Fig. 5.** Left figure: All LEAM HK data: 10 measurements in channels 83 and 84. Five different measurements are sub-commutated in each channel. The five channels of HK word 83 (blue) are from top to bottom (value at lunar night): +5 V Supply, Power Supply Monitor, Bias Voltages Monitor, and both Sensor Dust Covers Status and Mirror Dust Cover Status on top of each other at  $\sim 0$  DN value (both covers were open since LEAM's first lunation on the Moon). The five channels of HK word 84 (red) are  $-5$  V Supply at DN value  $\sim 230$  and the temperature measurements from top to bottom (value at lunar night): Central Electronic Temp, West Microphone Temp, East Microphone Temp, Up Microphone Temp. Right figure: relationship between LEAM Electronics Survival Temperature and Central Electronic Temperature. The periods when the Electronics Survival Temperature was  $> 187$  are shaded yellow. (For interpretation of references to color in this figure legend, the reader is referred to the web version of this article.)

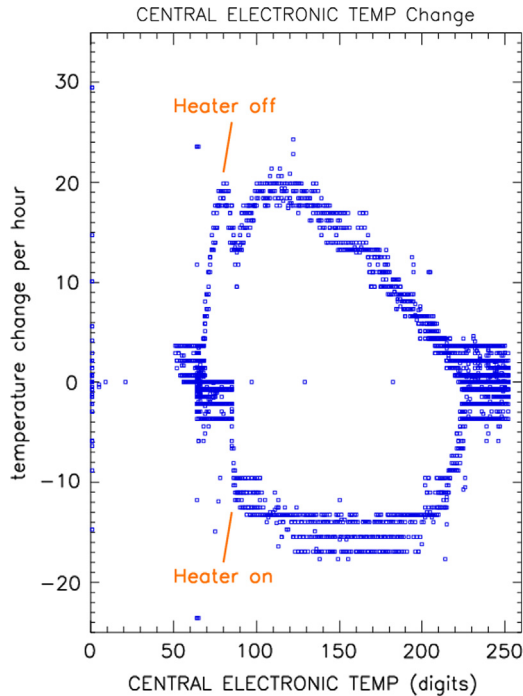


**Fig. 6.** Hysteresis of LEAM Central electronics temperature. The temperature change (DN) per hour is plotted vs. the temperature (DN). Heater switch-off occurred at  $\sim 80$  DN, heater switch-on at  $\sim 90$  DN.

Despite the similarities in the trend of LEAM temperatures there are small differences. At sunrise the East Sensor temperature rises faster than West Sensor, and at sunset the East Sensor temperature falls faster than the West Sensor temperature. Both the Central electronics and open West sensor show effects of the

heater: kinks in the morning temperature rise between 70 and 80 DN values and the sudden reduction in the evening temperature decline. The closed (by front-films) Up and East sensors show no clear effects of the heater. The heater switching is quite obvious in the temperature hysteresis of the Central Electronics temperature (Fig. 6). The temperature gradient is reduced when the heater was switched-off and, conversely, when the heater was switched-on. During nighttime the temperature was very stable at low levels ( $\sim -25$  °C) with no indication of any temperature control.

The Heater Status bit in the science frame is very noisy and displays frequent random fluctuations (several per day) that have no relation to actual heater status as indicated by temperature profile.

No comprehensive technical handbook of the LEAM instrument was available to us. The most detailed description of the LEAM instrument available was Berg et al. (1973), and some uncertainties remain in our interpretation of the data. Uncertainties that could not be resolved with the information available to us are

- the conversion of LEAM HK channels to physical quantities,
- the identification of the strips that contain the controls on the East Sensor and on the West Sensor,
- the nominal values of the Test Pulses, and
- the Sun altitude above the local horizon.

## 7. Science data analysis

In a first step we calculated the sum of all LEAM science channels (Fig. 7). The times when the instrument shuts-off are clearly identified as the sum reaches the maximum total value of  $\sim 369$ . During the times when the instrument was switched on there were peaks in the sum of all science data  $> 200$  DN that were regularly spaced, these peaks were identified as test signals

(see below). During a total period of 77 days and 3 h the instrument temperature (Fig. 4) was lower than 60 °C. We flag the periods when the temperature was above 60 °C (Fig. 7). The original LEAM investigators did not report on any useful results from the four microphones on board, and we did not look deeper in this data.

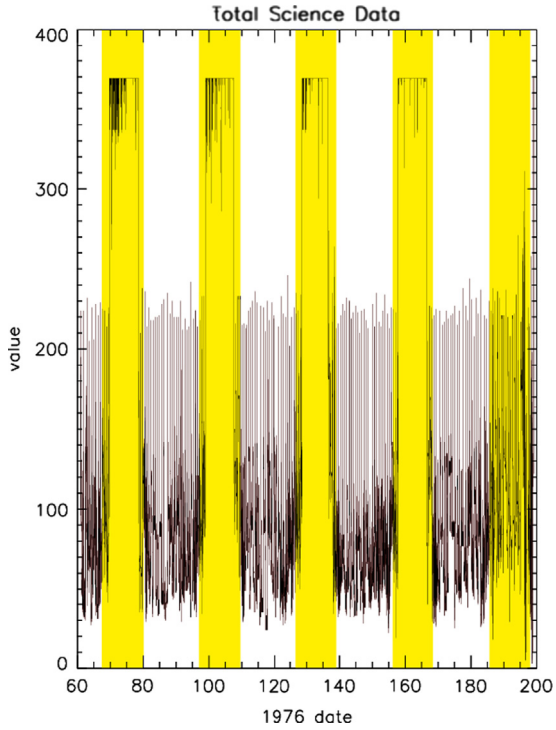
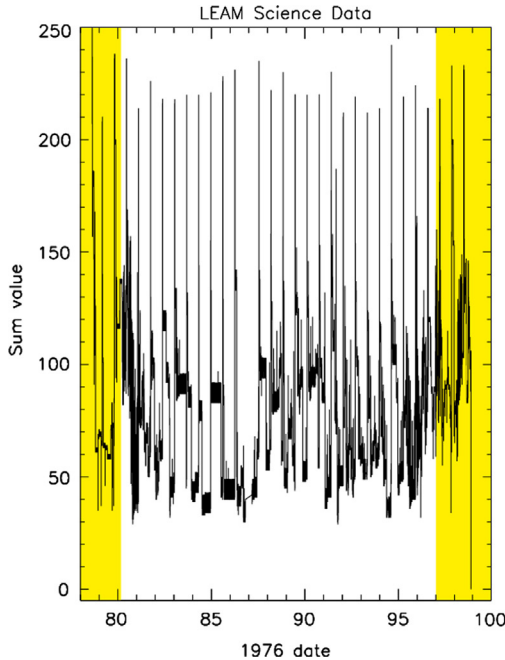


**Fig. 7.** Total science data during normal operation. The total science value is the sum of all channels in one LEAM Science Data Set (Table 2). The yellow shaded bars indicate periods when LEAM temperatures were higher than  $\sim 60^{\circ}\text{C}$  during lunar noon. (For interpretation of references to color in this figure legend, the reader is referred to the web version of this article.)



## 8. Test pulses

Before we can interpret the LEAM science data test pulses have to be extracted from the data set. There are two ways to identify test pulses in the LEAM data set (Fig. 8):

- (1) by the total of all science channels, because all IDs are 15, all or most film strips are triggered, and elapsed times are  $> 25$ ; and
- (2) by the number of new DN values between 18 and 24 in the individual channels, because most electronic channels were triggered by a test pulse.

At times of enhanced noise rates, especially during the later high temperature periods more events can satisfy these conditions which are obviously not automatic or commanded test pulses. Test pulse data sometimes extend over two science read-outs, probably because of some time delays between the test pulses onto the different sensors and the subsequent data processing. The automatic test pulses are about 15.4 h apart. Table 6 gives the DN values of the observed test data.

We observe the following anomalies in the Test Pulse data for which we do not have an explanation:

- No PHA measurement showed alternating small and big values for small and big test pulses.
- Three test pulse amplitudes (Sensor 1 channel 1 Front Film PHA, Sensor 3 channel 24 Film PHA, and channel 29 Main Microphone PHA) were systematically = 0 because either the corresponding test pulse generators failed or the test signals were so small that they triggered the corresponding ID and Accumulators but the pulse heights were still below the first level. At other times when channels 1, 24, and 29 were triggered by noise or impact events these channels generated PHA signals bigger than 0 which indicates that the PHA electronics did not fail.
- Sensor 1 channel 6 Front Collector ID systematically had the value of 12 DN, i.e. only film strips 3 and 4 triggered instead of all channels = 15 DN.
- Sensor 3 channel 23 Collector ID did not trigger.

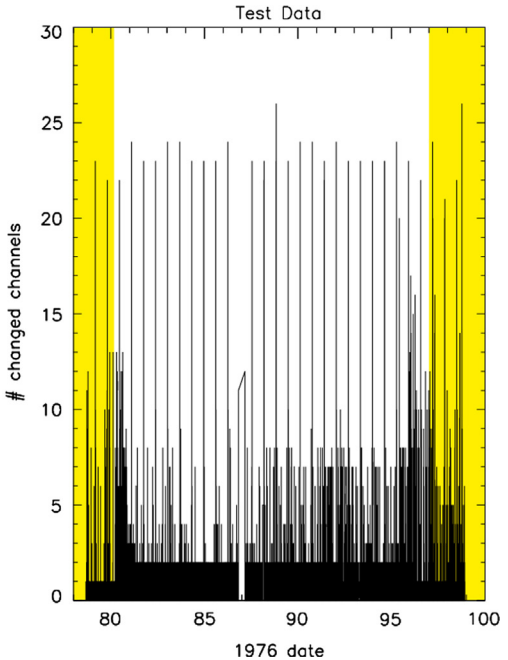


**Fig. 8.** Identification of test pulses during the 2nd lunation in 1976. Test pulses are identified by the sum of all science channels  $> 200$  (left) and by the number of changed channels  $> 20$  within two subsequent data read-outs ( $\sim 6$  s, right).

**Table 6**

Test pulse values of the different channels.

Channel	Meas. no.	UP Sensor 1	
		Measurement name	Test
0	DJ-1	Front film ID	15
1	DJ-2	Front film PHA	0
2	DJ-3	Front film accumulator	Var.
3	DJ-4	Rear film ID	15
4	DJ-5	Rear film PHA	5
5	DJ-6	Rear film accumulator	Var.
6	DJ-7	Front collector ID	12
7	DJ-8	Microphone PHA	6
8	DJ-9	Microphone accumulator	Var.
9	DJ-10	Rear collector ID	15
10	DJ-11	Elapsed time	> 25
<b>EAST Sensor 2</b>			
11	DJ-12	Front film ID	15
12	DJ-13	Front film PHA	4
13	DJ-14	Front film accumulator	Var.
14	DJ-15	Rear film ID	15
15	DJ-16	Rear film PIIA	5
16	DJ-17	Rear film accumulator	Var.
17	DJ-18	Front collector ID	15
18	DJ-19	Microphone PHA	4
19	DJ-20	Microphone accumulator	Var.
20	DJ-21	Rear collector ID	Var.
21	DJ-22	Elapsed time	> 33
<b>WEST Sensor 3</b>			
22	DJ-23	Film ID	3
23	DJ-24	Collector ID	0.3
24	DJ-25	Film PHA	0
25	DJ-26	Film accumulator	Var.
26	DJ-27	Secondary microphone accum.	Var.
29	DJ-30	Main microphone PHA	0
30	DJ-31	Main microphone accumulator	Var.

Var.: various values; mostly accumulators.

## 9. Noise rates

Dust impacts should show-up as coincident signals on both front film and front collector channels. Therefore, the individual trigger of only one channel is considered a noise event. During lunar night the noise rates of individual LEAM channels are a few times 10 events per 24 h (Fig. 9). The rates increase towards morning and reach about 100 per day after sunrise. However, Sensor 2 has two very noisy channels that trigger at an anomalously high rate: Channel 13 (DJ-14) Front Film Accumulator and channel 20 (DJ-21) Rear Collector ID. The latter is picking up interfering signals at a rate of one trigger per approx. 270 s which corresponds to the read-out of 90 LEAM science data sets or one complete LEAM HK data set (cf. Table 4). The signals show up as DN values increased by 2 (which indicates that Rear Collector strip 2 picked-up the interference) for 18 read-out steps ( $\sim 54$  s) after which the previous DN value returns. The Front Film Accumulator is stepping up at the same rate, which indicates that it picks-up the same interference. This interference has the effect that there are frequent accidental coincidences between film and grid signals which consequently increase the noise rate on both front and rear sensors of Sensor 2.

## 10. Candidate and potential dust events

Impacts of dust particles have the signature that both the front film and grid (collector) channels record in coincidence the charge

signals which advance the front film accumulator by one. In addition both the front film ID and front collector ID indicate which sensor element was hit (cf. Table 1) neither values should be 0. For big impacts multiple strips can trigger, and also a Front Film Pulse Height PHA is measured. Both high-speed impacts and impacts of slow highly-charged particles will have this signature. We will call these Front Film Grid (FFG) events. FFG events can be recorded by Sensors 1 and 2. Sensor 3 (West Sensor) will record these types of events by its rear sensor (RFG). As a first step we search the LEAM data from all sensors for such coincident **candidate dust events**. In a second step we will determine which of the candidate dust events qualify as **potential dust events**.

High-energy dust particles that penetrate the front film and impact on the rear film sensor are called Time-of-Flight (TOF) events. All corresponding channels of the front and rear sensor should respond as described above and, in addition, an Elapsed Time measurement between start and stop will also be recorded. While the Pioneer 8 and 9 instruments recorded several such TOF impacts, no TOF event was reported from LEAM during the first 22 lunations (Berg et al., 1975).

The rear collectors (RFG) of Sensors 1 and 2 should only respond to dust impacts when a simultaneous FFG event is also recorded by a corresponding front sensor. Nevertheless, several RFG only events have been recorded by LEAM during the 1976 period (Table 7). Fig. 10 shows the occurrence of candidate dust events in the different data blocks (lunations in 1976). The number of candidate dust events is low during lunar nights. However, during periods of excessive heating the occurrence of such events is much higher and they come in bursts. Even during times when the LEAM temperature is below  $\sim 60$  °C sometimes candidate dust events are registered in bursts.

In order for candidate dust events to be qualified as "potential dust events" we must have a closer look at the individual channels of each coincident event (Table 8).

There are a number of obvious anomalies in the list of candidate dust events (Table 8).

1. Only FFG1, FFG2, and RFG3 events can be caused by dust particles, both slow or fast ones.
2. On day 96.024526 Sensor 2 recorded a TOF event: both FFG2 and RFG2 responded simultaneously with an elapsed time measurement of 14 DN.
3. Other Rear Sensor events RFG1 and RFG2 cannot be caused by dust particles. Therefore, all those rear sensor events of Sensors 1 and 2 are removed from the list of candidates. The LEAM investigators did not report any Rear Sensor only events on Sensors 1 and 2. We have not looked into the details of these Rear Sensor only events.
4. On day 95.9 Sensor 3 RFG3 recorded a burst of new events with all the same parameters (F-ID, PHA, ACC, and C-ID). These are not just repetitions of the same data set since the preceding data set was quite different and the accumulator advanced. Therefore, we had a closer look at this burst of RFG3 events. However, a long list of subsequent data read-outs showed that this data set toggled between two different states (Table 9). This sequence cannot be caused by dust impacts; therefore, all but one event are removed from the list of candidates. Other smaller bursts of similar events on the same sensor do not show an obvious sign of faulty data.

After removal of the obvious non-dust events from the list, 19 potential dust events (Table 10) and one TOF event (Table 11) remain in the record of sensors 1, 2, and 3 during the 5 lunations in 1976 when the instrument was at moderate temperatures.

The 19 events recorded during a total 74.6 days, when LEAM was expected to operate nominally having a temperature below

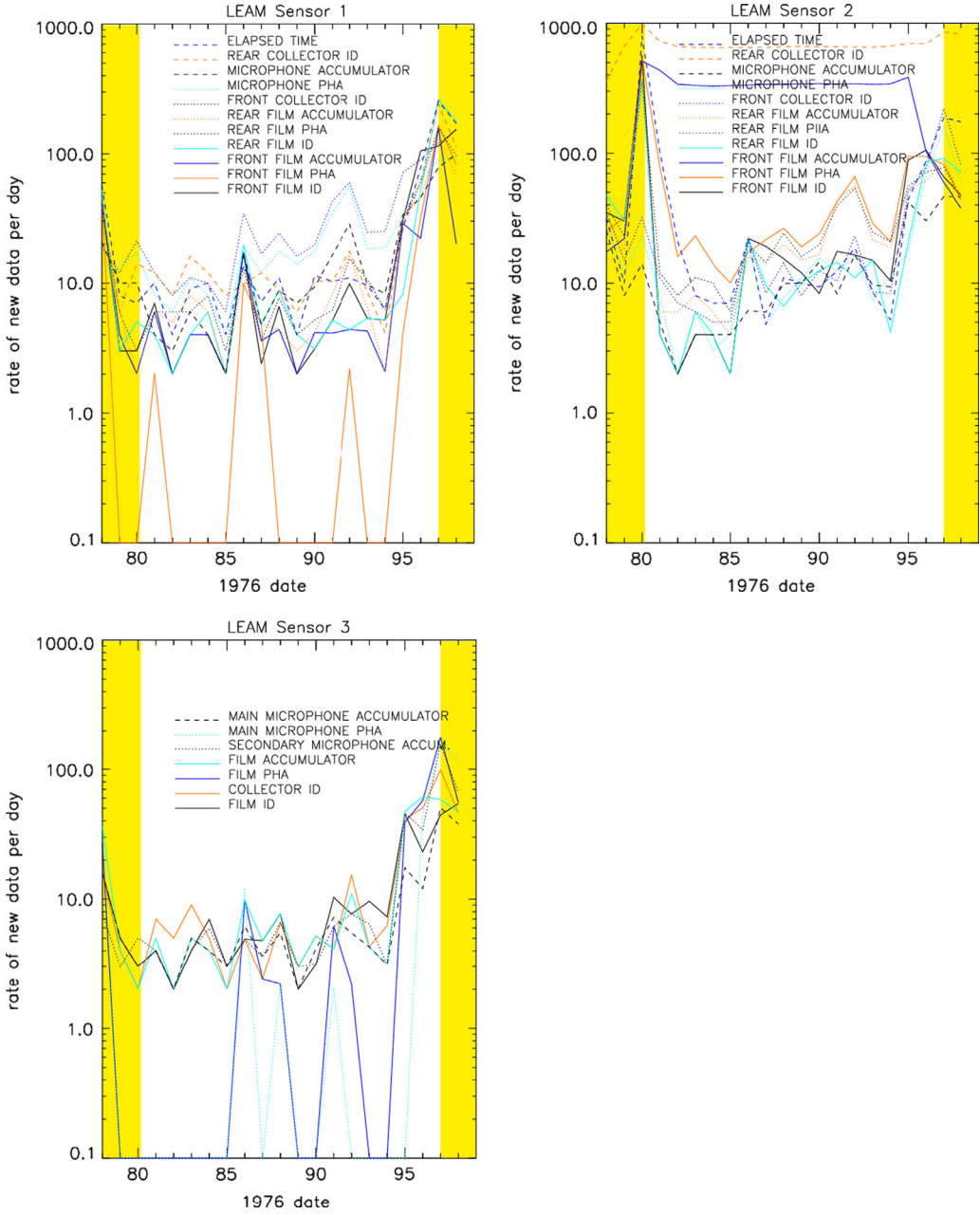


**Fig. 9.** Noise rate of individual channels of UP Sensor 1 (upper left), EAST Sensor 2 (upper right), and WEST Sensor 3 (below) during the 2nd lunation in 1976. Sensor 2 Front Film Accumulator and Rear Collector ID show continuous high rate activity at a rate of 1 and 2 events per 4.5 min, respectively.

**Table 7**

Number of recorded candidate events in the different data blocks (lunations in 1976). Both events recorded by UP Sensor 1 (front sensor FFG1, rear sensor RFG1, and Time-of-flight TOF1), EAST Sensor 2 (FFG2, RFG2, TOF2), and WEST Sensor 3 (only RFG3). TP is the number of test pulses.

	FFG1	RFG1	TOF1	FFG2	RFG2	TOF2	RFG3	TP
<b>Block 1</b>	0	0	0	0	0	0	2	3765
<b>Block 2</b>	1	1	0	4	12	1	16	13,569
<b>Block 3</b>	1	1	0	0	11	0	7	11,777
<b>Block 4</b>	30	23	0	14	10	0	54	22,938
<b>Block 5</b>	53	59	0	27	48	0	69	61,395
<b>Sum</b>	85	84	0	45	81	1	148	113,444

60 °C, indicates an average event rate of  $\mu \sim 0.25/\text{day}$ . Fig. 11 shows the cumulative distribution of the fraction hits as function of the elapsed time using the data from the rightmost column of

**Table 10.** For a uniform random distribution of  $N$  events during a period  $T$ , the average rate is  $\mu = N/T$ , and the cumulative probability of finding all the events separated by a period of  $< t$  is  $P(< t) = 1 - e^{-\mu t}$ . The deviation from this trend indicates clustering in time of the recorded hits. For example, assuming that half the hits happened at a different rate, the cumulative probability distribution can be approximated as  $P(< t) = 0.5(1 - e^{-\mu_1 t}) + 0.5(1 - e^{-\mu_2 t})$ . Setting  $\mu_1 = \mu/2$  and  $\mu_2 = 100\mu$ , greatly improves the fit to LEAM observations. Indeed about half of the hits occurred within about 1 h or less after each other on the same sensor. Three hits were recorded about 5 days after sunset on day 114.36 by Sensor 3 even within minutes after each other. Weaker bursts (about an hour separation between subsequent hits) were recorded by Sensors 2 and 3 (West Sensor) on days 96.0 and 147.3. Both bursts occurred within the middle of lunar night.

The event rate of potential dust events during 5 lunations covered by the 1976 LEAM data is shown in Fig. 12. Events

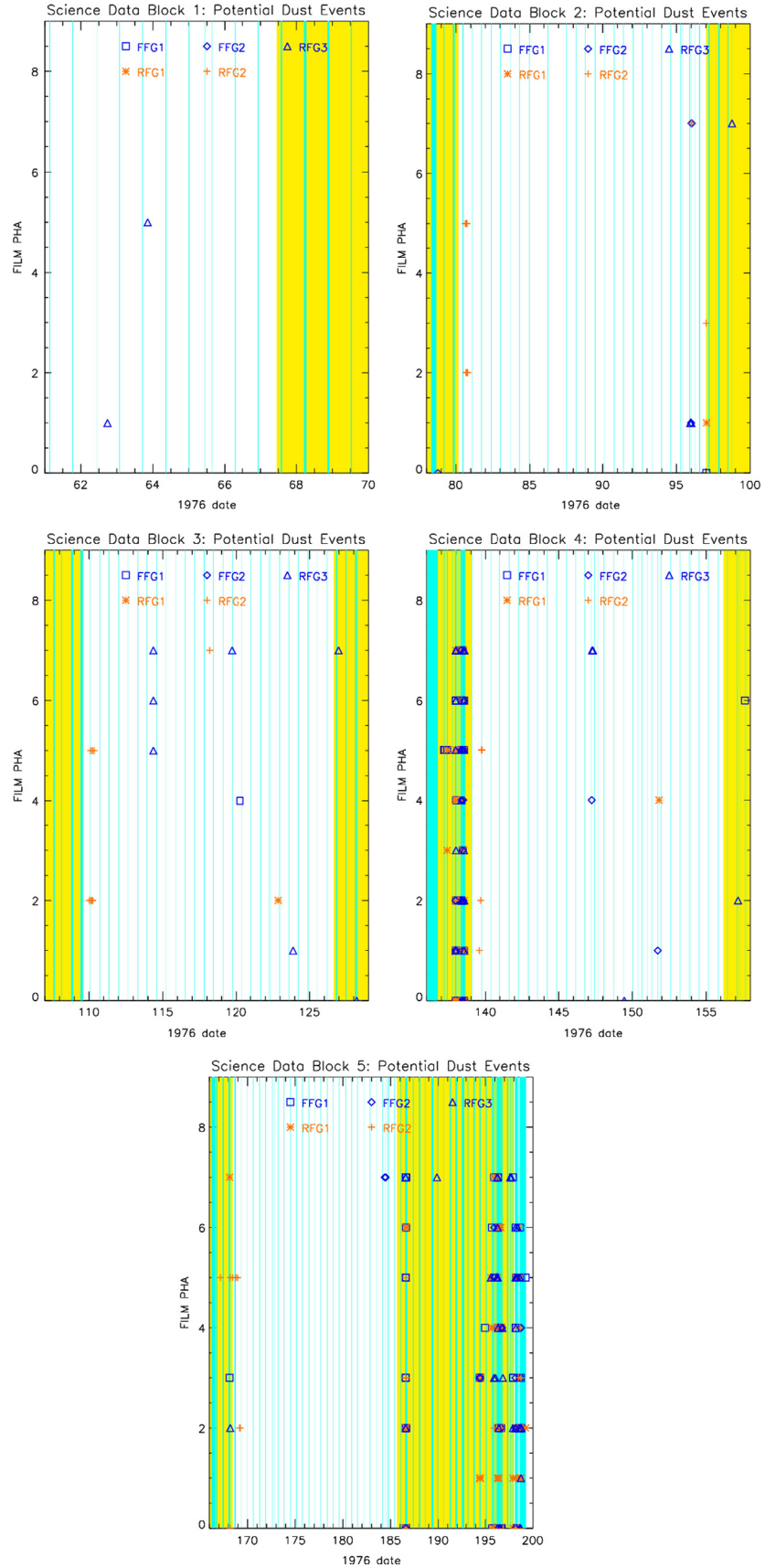


**Fig. 10.** Pulse height amplitudes of candidate (coincident) dust events in the 5 different data blocks (lunations in 1976). The different types of events are marked (blue: front sensors FFG events and red: rear sensors RFG events) and the sensor numbers are given. Sensor 3 RFG3 is not covered by a film and can record low-energy and slow dust impacts, therefore, it is marked blue. The turquoise vertical lines mark the times when test pulses have been recorded. Periods of excessive heating are shaded yellow. The rate of candidate dust events is low during lunar night. Bursts of coincident events occur mostly during times when the LEAM temperature exceeded 60 °C. (For interpretation of references to color in this figure legend, the reader is referred to the web version of this article.)

**Table 8**

Candidate dust events during times when the LEAM temperature was below 60 °C. The columns are: type which refers to the sensor element (FFG: Front Film Grid; RFG: Rear Film Grid) and sensor number; decimal day in 1976; and measurement parameters (F-ID: Film ID; PHA: Pulse height; ACC: Accumulator; and C-ID: Collector ID).

Type	Day	F ID	PHA	ACC	C ID	Type	Day	F ID	PHA	ACC	C ID
RFG3	62.739430	1	1	6	1	RFG2	110.143072	5	2	5	10
RFG3	63.854850	1	5	1	3	RFG2	110.155895	5	2	5	10
RFG2	80.631987	10	5	2	8	RFG2	110.218543	10	5	2	2
RFG2	80.679785	5	2	4	8	RFG2	110.231122	5	2	5	2
RFG2	80.681148	10	5	2	10	RFG2	110.231716	10	5	2	2
RFG2	80.693482	5	2	4	8	RFG2	110.249989	5	2	5	10
RFG2	80.699841	10	5	2	8	RFG2	110.347997	10	5	2	2
RFG2	80.707842	5	2	4	8	RFG3	114.362065	3	7	6	3
RFG2	80.712594	5	2	4	2	RFG3	114.363288	3	5	2	2
RFG2	80.727514	5	2	4	8	RFG3	114.364155	3	6	2	2
RFG2	80.744704	10	5	2	8	RFG2	118.180660	15	7	7	3
RFG2	80.794355	5	2	4	10	RFG3	119.706586	3	7	5	2
RFG3	95.947379	2	1	6	2	FFG1	120.260768	1	4	5	8
RFG3	95.955974	2	1	6	2	RFG1	122.873609	4	2	0	4
RFG3	95.956673	2	1	6	2	RFG3	123.887632	3	1	6	2
RFG3	95.957266	2	1	6	2	RFG2	139.575600	8	1	2	2
RFG3	95.957686	2	1	6	2	RFG2	139.661414	5	2	5	8
RFG3	95.958734	2	1	6	2	RFG2	139.720253	10	5	2	2
RFG3	95.961599	2	1	6	2	RFG2	139.737968	10	5	2	8
RFG3	95.961983	2	1	6	2	RFG2	139.743908	10	5	0	8
RFG3	95.962228	2	1	6	2	FFG2	147.237093	14	4	6	6
RFG3	95.962997	2	1	6	2	RFG3	147.262320	3	7	6	3
RFG3	95.973828	2	1	6	2	RFG3	147.305436	3	7	5	3
RFG3	95.978230	2	1	6	2	RFG3	147.317210	3	7	6	3
RFG3	95.980746	2	1	6	2	RFG3	149.443091	3	0	3	2
RFG3	95.990844	2	1	6	2	FFG2	151.713695	1	1	2	4
FFG2	95.992661	8	1	5	8	RFG1	151.803910	8	4	0	8
RFG3	95.993499	2	1	6	2	RFG2	168.803995	10	5	2	10
FFG2	96.024526	7	7	7	10	RFG2	168.967656	10	5	2	2
RFG2	96.024526	15	7	7	9	RFG2	169.170939	5	2	4	8
FFG2	96.032143	15	7	7	10	RFG2	169.237116	5	2	4	8
RFG2	110.023576	5	2	5	10	FFG2	184.389527	15	7	7	8
RFG2	110.100724	10	5	2	8	FFG2	184.499518	3	7	7	10
RFG2	110.136782	5	2	5	2						

**Table 9**

Sequence of data read-outs of Sensor 3 RFG3 parameters (cf. Table 7).

Day	F ID	PHA	ACC	C ID
95.961529	3	0	5	0
95.961564	3	0	5	0
95.961599	2	1	6	2
95.961634	2	1	6	2
95.961913	3	0	5	0
95.961948	3	0	5	0
95.961983	2	1	6	2
95.962018	3	0	5	0
95.962158	3	0	5	0
95.962193	3	0	5	0
95.962228	2	1	6	2

recorded during times of excessive heating (yellow bars) have not been corrected for noise contributions. There is a very low event rate during lunar night and no significantly enhanced event rate around sunrise and sunset can be seen. Higher rates of candidate events were recorded during times of excessive heating.

All recordings added up for the three LEAM sensors are shown in Fig. 13. UP Sensor 1 recorded only 1 potential dust event between sunset and sunrise. The number and rates of candidate events was much higher during the day at times of excessive heating. EAST Sensor 2 recorded 7 potential dust events during lunar night including a single TOF event at sunrise. The number of candidate events was higher in the afternoon than in the morning hours. WEST Sensor 3 recorded 11 potential dust events spread

over during the night. Again the number of candidate events was high in the afternoon hours on this sensor as well. No significantly enhanced count rates were observed by either sensor around the time of sunrise and sunset.

## 11. Summary and conclusions

The LEAM instrument was exposed to strong variations in environmental conditions. Excessive heating was observed from about 24 h after sunrise until about 24 h before sunset. For about 9 days around lunar noon the temperatures were so high that LEAM was switched off. Only during the last lunation in 1976 LEAM stayed on. However, during the times of excessive heating LEAM became very noisy and no detailed analysis of the data has been executed as of yet. During the lunar night when the temperature were quite stable at ~−25 °C, and during the early morning and late afternoon, the instrument was stable and fairly quiet. One TOF event and 19 potential dust events (on the front sensors only) were recorded by all three sensors during a period of 77 days and 3 h when the instrument was at moderate temperatures. However a similar number of events were recorded on the rear sensor only. The latter events cannot be explained by dust impacts.

Of the 19 potential dust events nine are compatible with a random occurrence (~ one per week) the other 10 events occurred in three statistically significant bursts within about 1 h or less after each other. Two bursts occurred within the middle of lunar night when both Sensors 2 and 3 recorded a few hits. One burst of three events within minutes of each other was recorded by the (West) Sensor 3 just an hour before sunrise. Only during the lunar days when the instrument was heated beyond ~60 °C the numbers and the rates of candidate events were higher.

Although the rates of LEAM data from 1976 in Fig. 13 look qualitatively similar to the rates from 1973 and 1974 in Fig. 3 from Berg et al. (1975) the relation of the peak fluxes to the times of sunrise and sunset are quite different. The peak rates in 1976 occur about 50 h before sunset and after sunrise, respectively, at times when the instrument temperatures were already beyond the calibrated range and the noise rates at all channels were strongly enhanced. The bursts of such events on both front and rear sensors are probably either instrumental interferences or caused by local effects (solar flares, energetic particles, near-by micrometeoroid impacts, etc.). During the 1976 period the LEAM instrument showed severe degradation. Especially after the last baking during lunar noon with the instrument powered up the LEAM instrument did not provide any data useful to us.

Nevertheless, most of the sporadic front sensor events FFG1, FFG2, and RFG3 that were recorded when the instrument was at moderate temperatures look reasonable as expected from dust impacts and especially the Time-Of-Flight event TOF2 has attributes of a true high-velocity dust impact. The pulse heights of the potential dust events are high and many have the maximum pulse height value of 7. These characteristics of lunar dust data were already reported by Berg et al. (1976). The TOF event was probably caused by a fast and big particle of interplanetary origin since the elapsed time between front and rear sensor was less than one fourth (14 DN) of the maximum value (63 DN), both front and rear sensor recorded maximum PHA of 7, and multiple sensor strips responded to the impact as expected.

In interplanetary space at 1 AU from the sun the similar instruments on Pioneers 8 and 9 recorded about 300 FFG events and 20 TOF events over a period of about 7 years which represent a flux of  $8.2 \times 10^{-4} \text{ m}^{-2} \text{ s}^{-1}$  (per  $2 \pi$  steradian) of FFG-type particles and  $2.2 \times 10^{-4} \text{ m}^{-2} \text{ s}^{-1}$  of TOF-type ( $m \sim 10^{-13} \text{ g}$ ) particles (Berg and Grün, 1973). The Pioneer 8 and 9 fluxes showed

**Table 10**

Potential dust events during times when the LEAM temperature was below  $\sim 60$  °C (cf. Table 7). Additionally the time periods during which these events were observed are indicated; also the times between consecutive events are given.

Block	Total ops. time [h]	Type	Day	F ID	PHA	ACC	C ID	Time before LEAM temperature reached $-20$ °C [day]	Time between events [h]
1	154.8	RFG3	62.739430	1	1	6	1	3.74657	26.7700
		RFG3	63.854850	1	5	1	3	2.63115	
2	404.4	RFG3	95.947379	2	1	6	2	0.095621	1.0867
		FFG2	95.992661	8	1	5	8	0.050339	
		FFG2	96.032143	15	7	7	10	0.010857	0.9475
3	408.528	RFG3	114.362065	3	7	6	3	11.191935	0.0292
		RFG3	114.363288	3	5	2	2	11.190712	
		RFG3	114.364155	3	6	2	2	11.189845	0.0208
		RFG3	119.706586	3	7	5	2	5.847414	128.2183
		FFG1	120.260768	1	4	5	8	5.293232	13.3002
		RFG3	123.887632	3	1	6	2	1.666368	87.0448
4	411.048	FFG2	147.237093	14	4	6	6	7.476907	0.6053
		RFG3	147.262320	3	7	6	3	7.45168	
		RFG3	147.305436	3	7	5	3	7.408564	1.0349
		RFG3	147.317210	3	7	6	3	7.39679	0.2827
		RFG3	149.443091	3	0	3	2	5.270909	51.0208
		FFG2	151.713695	1	1	2	4	3.000305	54.4947
5	412.848	FFG2	184.389527	15	7	7	8	0.126473	2.6396
		FFG2	184.499518	3	7	7	10	0.016482	

**Table 11**

The single time-of-flight (TOF) dust event recorded by Sensor 2 front and rear sensor simultaneously.

Type	Day	Front sensor				Rear sensor				TOF
		F ID	PHA	ACC	C ID	F ID	PHA	ACC	C ID	
TOF2	96.024526	7	7	7	10	15	7	7	9	14

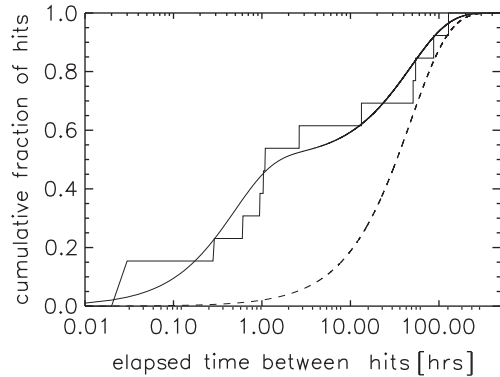


**Fig. 11.** The cumulative fraction of the total number of hits as function of the elapsed time between events. The expectation for uniformly randomly distributed events is shown by the dashed line. The smooth line shows the expectation assuming that half the events happened at a rate 100 times higher than the average.

a strong dependence on the viewing direction of the dust sensor during a spacecraft spin: most of the smallest FFG events were observed from the solar direction while the bigger FFG and the TOF events arrived from predominantly the apex direction (Berg and Grün, 1973). The LEAM instrument on the moon has a similar measurement configuration and sensitivity as the Pioneer 8 and 9 detectors: during one lunation the viewing directions of the different sensors roughly scan through the interplanetary dust flux along the ecliptic plane where the noon shut-off interrupts the scan. The Pioneer fluxes translate into  $\sim 50$  FFG and  $\sim 15$  TOF events over the total period of 77 days and 3 h when the instrument temperature was lower than 60 °C. However, if one considers that the field-of-view of the LEAM East and West sensors

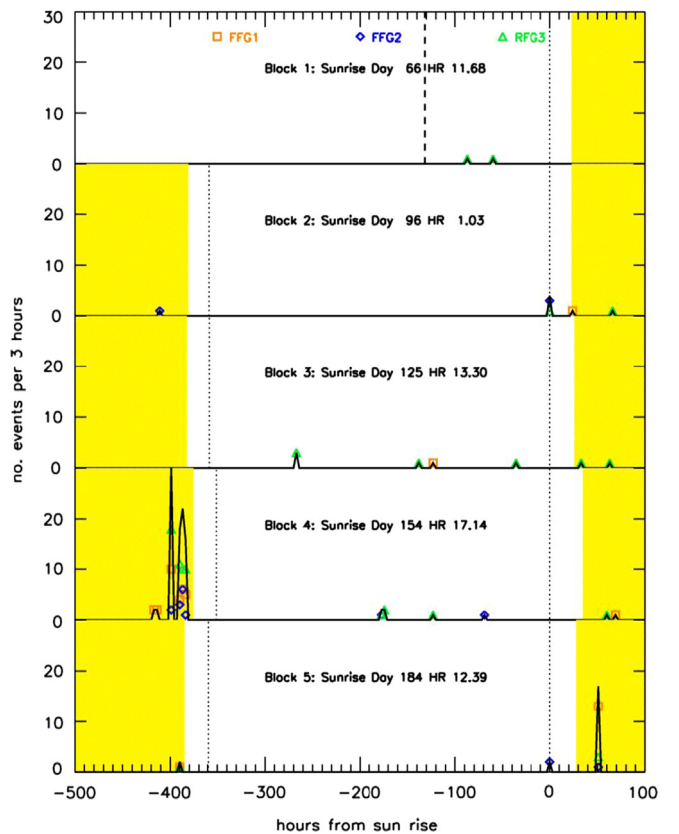


**Fig. 12.** Number of potential dust events per 3 h period for 5 lunations in 1976 (data blocks) covered by the data. Events on different sensors are marked by different symbols. Yellow shaded bars represent times of excessive heating. Sunrise and sunset are marked by dotted lines. Events recorded during times of excessive heating have not been corrected for noise contributions. The dashed line represents the beginning of the data set. (For interpretation of references to color in this figure legend, the reader is referred to the web version of this article.)

is reduced to  $< 50\%$  by the surrounding terrain the expected numbers of dust events are close to what has been observed. Therefore, we conclude that the LEAM nighttime dust measurements are compatible with measurements of interplanetary meteoroids by the Pioneer

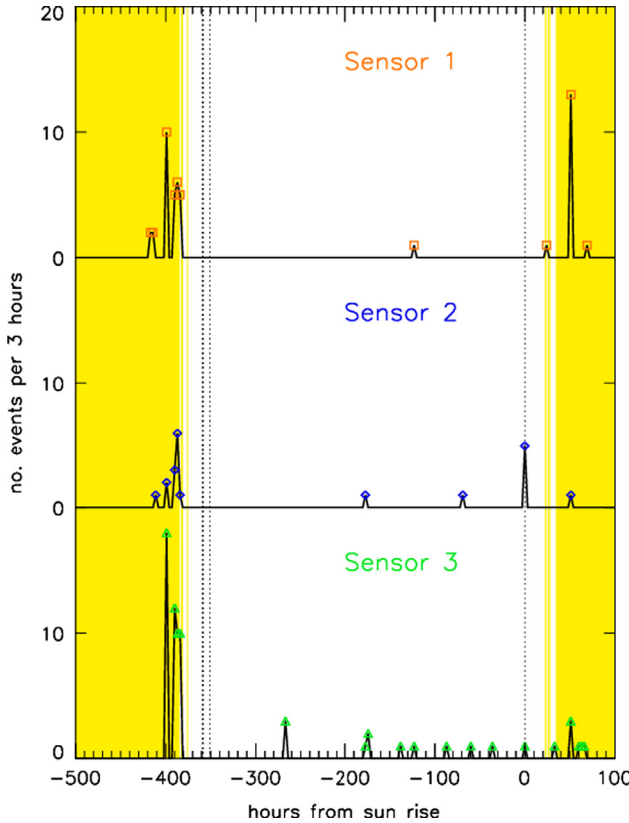


**Fig. 13.** Number of potential dust events per 3 h period for the three LEAM sensors. Yellow shaded bars represent start and end times of excessive heating. Sunrise and sunset are marked by dotted lines. Events recorded during times of excessive heating were not corrected for noise contributions. (For interpretation of references to color in this figure legend, the reader is referred to the web version of this article.)

8 and 9 dust instruments. A few bursts of potential dust events may be due to ejecta from distant primary meteoroid impacts onto the lunar surface.

The criticism of O'Brien (2011) could not be supported by our analysis of the 1976 LEAM data. The parameters of the potential dust events have all attributes of true dust impacts and especially the single TOF event is most probably of interplanetary origin. There is no systematical correlation between the recorded signals and the two switches (on and off) of the LEAM heater that occurred per lunation in 1976. It is true that the majority of observed signals occurred in bursts especially during times of excessive heating. During the quiet night times half of the events are sporadic events that do not show strong clustering. Three bursts have been identified that occurred within a period of a few hours.

There is a gap of about 16 months ( $\sim 16$  lunations) between the last data reported by the LEAM investigator (Berg et al., 1975) and the data available to us. Therefore, the instrument performance

may have changed sufficiently to explain the differences between the results obtained here and those reported earlier. The 1976 LEAM nighttime data do not support significantly enhanced dust activity near the terminator while the high pulse amplitudes of lunar dust events is confirmed. Additional in depth analysis of the 1976 daytime measurements by LEAM and especially of data from other periods may provide more insight into the behavior of LEAM on the lunar surface.

The precursor Pioneer 8 and 9 dust instruments successfully characterized the interplanetary dust environment. However, the harsh environmental conditions on the lunar surface prohibited a similar success of the LEAM instrument. New information on the lunar dust environment will come from the LDEX instrument (Horányi et al., 2012) orbiting the moon on the LADEE satellite but final confirmation or rejection of some LEAM results (Grün et al., 2011) needs a more sensitive and robust instrument on the lunar surface.

## Acknowledgment

This work was supported by NASA Lunar Science Institute's funds to the Colorado Center of Lunar Dust and Atmospheric Studies. The authors thank Dr. Yosio Nakamura for providing access to the LEAM data and for his help in deciphering it. Valuable information and comments were given by Lynn Lewis, Chairman of NASA Lunar Science Institute Focus Group on Recover of Missing ALSEP Data. The authors thank Ralf Srama and Brian O'Brien for helpful comments.

## References

- Anon., 1975a. Apollo Scientific Experiments Data Handbook, NASA TM X-58131.
- Anon., 1975b. Apollo Lunar Surface Experiment Package Archive Tape Description Document, JSC-09652.
- Anon., 1972. Apollo Lunar Surface Experiments Package. Apollo 17 ALSEP (Array E) Familiarization Course Handout, NASA-CR-128636, Bendix Corp.
- Bailey, C.L., Frantsvog, D.J., 1976. Response of the LEAM detector to positively charged microparticles (NASA contract no. NASS-23557). Concordia College.
- Berg, O.E., Grün, E., 1973. Evidence of hyperbolic cosmic dust particles. *Space Res.* XIII 2, 1047–1055.
- Berg, O.E., Richardson, F.F., 1969. The Pioneer 8 cosmic dust experiment. *Rev. Sci. Instrum.* 40, 1333–1337.
- Berg, O.E., Richardson, F.F., Burton, H., 1973. Lunar Ejecta and Meteorites Experiment (Apollo 17 preliminary science report, NASA SP-330,16).
- Berg, O.E., Wolf, H., Rhee, J.W., 1975. Lunar soil movement registered by the Apollo 17 cosmic dust experiment. In: Interplanetary Dust and Zodiacal Light, Lecture Notes in Physics, vol. 48, 233.
- Grün, E., Berg, O.E., Dohnanyi, J.S., 1973. Reliability of cosmic dust data from Pioneers 8 and 9. *Space Res.* XIII, 1057–1062.
- Grün, E., Horányi, M., Sternovsky, Z., 2011. The lunar dust environment. *Planet. Space Sci.* 59, 1672–1680.
- Horányi, M., Sternovsky, Z., Lankton, M., James, D., Szalay, J., Drake, K., Shu, A., Colette, A., Grün, E., Kempf, S., Srama, R., Mocker, A., 2012. The dust environment of the moon: expectations for the Lunar Dust Experiment (LDEX). In: Lunar and Planetary Institute Science Conference Abstracts, 43, 2635.
- O'Brien, B.J., 2011. Review of measurements of dust movements on the Moon during Apollo. *Planet. Space Sci.* 59, 1708–1726.
- Perkins, D., 1976. Analysis of the LEAM experiment response to charged particles (NASA contract no. NAS9-14751). Bendix Aerospace Systems Division, BSR 4233.